Precision atomic beam density characterization by diode laser absorption spectroscopy

Paul Oxley and Joseph Wihbey
Physics Department, The College of the Holy Cross, Worcester, Massachusetts 01610, USA

(Received 13 June 2016; accepted 20 August 2016; published online 2 September 2016)

We provide experimental and theoretical details of a simple technique to determine absolute line-of-sight integrated atomic beam densities based on resonant laser absorption. In our experiments, a thermal lithium beam is chopped on and off while the frequency of a laser crossing the beam at right angles is scanned slowly across the resonance transition. A lock-in amplifier detects the laser absorption signal at the chop frequency from which the atomic density is determined. The accuracy of our experimental method is confirmed using the related technique of wavelength modulation spectroscopy. For beams which absorb of order 1% of the incident laser light, our measurements allow the beam density to be determined to an accuracy better than 5% and with a precision of 3% on a time scale of order 1 s. Fractional absorptions of order 10^{-5} are detectable on a one-minute time scale when we employ a double laser beam technique which limits laser intensity noise. For a lithium beam with a thickness of 9 mm, we have measured atomic densities as low as 5×10^4 atoms cm^{-3}. The simplicity of our technique and the details we provide should allow our method to be easily implemented in most atomic or molecular beam apparatuses. *Published by AIP Publishing.* [http://dx.doi.org/10.1063/1.4962025]

I. INTRODUCTION

Collimated atomic and molecular beams have been used in experiments for almost as long as the field of atomic and molecular physics has existed.[1–4] They are used in a diverse range of areas of research including collision physics,[5–9] plasma physics,[10–16] laser cooling and atom beam lithography,[17–22] precision measurements,[23–27] and Rydberg atom research.[28–32]

A key parameter of the atomic or molecular beam is its density. For example, experiments which use beams as collision targets require knowledge of the beam density to determine absolute collision cross sections. Beam density is, however, difficult to measure accurately and with high precision. Laser-induced atomic fluorescence[33,34] measurements have been used to infer beam density and these measurements are straightforward to make experimentally. They are, however, prone to inaccuracies due to the difficulty of determining experimental parameters such as light collection efficiency. Ionization techniques[35,36] have also been used. These have the advantage that they are independent of the beam species atomic or molecular structure, but are destructive methods with limited precision. Using the above methods, typical uncertainties in measured densities are 15% or greater.

Indirect methods for determining beam density can also be employed. For molecular beams with room-temperature gasses, a measurement of the gas flow rate into the source apparatus is used to infer the beam density. Similarly, for heated oven beam sources such as those producing alkali metal atom beams, a vapor pressure curve can be used to infer the beam density once a measurement of the oven temperature has been made.[37,38] In this case, ensuring that the measured temperature accurately reflects the temperature of the source material can be challenging. In addition, the steep variation of vapor pressure with temperature gives large errors in pressure and therefore density, for relatively small errors in temperature.

Laser absorption spectroscopy of atomic beams is an alternative approach to directly measure beam density,[39–42] which can be more precise, and is the approach we take here. In our work, unlike in other laser absorption studies, we have confirmed the accuracy of our measurements using an independent technique and we provide an analysis of the precision of our measurements. Our method is simple to implement, is precise and sensitive, and can determine beam densities in real time. The technique involves chopping on and off an atomic beam which is intersected at right angles by resonant laser light. The laser power transmitted by the atomic beam is analyzed to infer the fractional absorption of light by the atoms and hence to determine the atomic beam density. The related technique of wavelength modulation spectroscopy (WMS)[43] is the technique we use to confirm our results and to estimate the accuracy of our method. To our knowledge, our work is the first example of WMS applied to a collimated atomic beam. We note that while chopping the atomic beam is undesirable for some applications, for other experiments (e.g., if the beam is used as a collision target), chopping provides a natural way to remove background signals not associated with the atomic beam. In addition, if one is satisfied with monitoring the beam density only periodically, then continuous chopping is not required.

II. EXPERIMENT

The experimental apparatus used to generate a lithium atomic beam and to measure its density is shown in Fig. 1. The atomic beam is produced by an oven in which lithium is

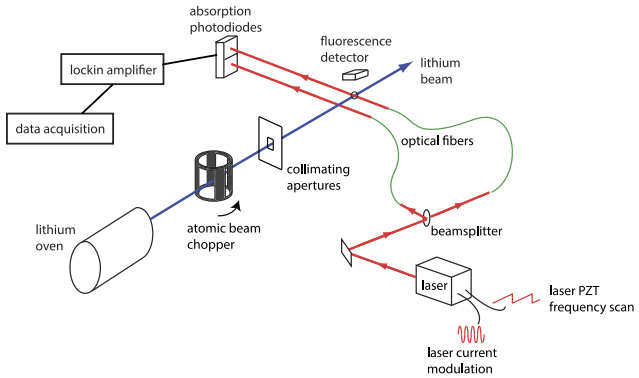

FIG. 1. Experimental setup used to measure lithium atomic beam density by laser absorption. Measurements using the chopped beam technique require that the atomic beam chopper is turning, but no laser current modulation is applied. The reverse is the case for measurements using the WMS technique. Of the two laser beams reaching the absorption photodiodes, only one passes through the lithium beam.

heated to a temperature of 465 °C by a set of four cartridge heaters which provide a total heating power of 140 W. Lithium vapor emerges from the oven through 67 nozzles, each 0.9 mm diameter, 9 mm long, and passes through a mechanical chopper and a series of apertures which collimate the lithium beam. The chopper is a 30.5 mm diameter cylinder with four slots cut along its length and is rotated about its axis at 21.75 Hz. This arrangement chops the atomic beam at a frequency of 87 Hz. An LED-photodiode pair monitors the chopper axle position and provides a reference for the lock-in amplifier used when measuring laser absorption (see below). At a distance of 60 cm from the oven exit and 42 cm from the chopper, the lithium beam is intersected at right angles by a laser beam used to probe the atomic density, integrated along the laser path. At this point, the atomic beam is approximately 15 mm tall and 9 mm thick, while the laser beam is circular with a diameter of 2.8 mm. The oven and atomic beam are located inside a vacuum apparatus in which the pressure is approximately 2×10^{-7} Torr.

The laser used is a grating-stabilized diode laser, the frequency of which is controlled by applying a voltage to a piezoelectric transducer (PZT) mounted on the diffraction grating, and also by the laser injection current. A 0.95 Hz saw-tooth voltage applied to the PZT scans the laser frequency across the $2S_{1/2}$, $F = 2 \rightarrow 2P_{3/2}$, $F = 1,2,3$ lithium resonance and when employing the WMS method, the laser current is modulated sinusoidally at a frequency of 9.5 kHz. The linewidth of the atomic transition is 50 MHz due to residual Doppler broadening of the collimated atomic beam. This linewidth is greater than the separation of the hyperfine structure intervals of the $2P_{3/2}$ state which are therefore unresolved in our experiments. The laser wavelength and frequency spectrum are continuously monitored by a wavemeter (BurleighWA-1000) and a scanning Fabry-Perot interferometer (Thorlabs SA200).

A double laser beam setup is implemented by using a beam splitter to divide the laser light into two separate beams, each of which is coupled into a single-mode optical fiber. Light from one of the fibers is passed through the lithium atomic beam and onto one channel (the "atoms channel") of a balanced photodiode pair (Thorlabs PDB210A), while light from the other fiber goes directly to the other photodiode channel (the "reference channel"). Absorption of laser light by the lithium beam results in an imbalance between the two absorption photodiode channels which can be used to infer the density of the atomic beam. The experiment can be performed with or without the reference channel present but including this channel reduces common mode noise, such as laser intensity noise, which is important when probing weakly absorbing atomic beams. The photodiode signal is fed to a lock-in amplifier whose output is recorded by an oscilloscope. When using the chopped atomic beam method to determine the atomic density, the reference for the lock-in amplifier is the 87 Hz chopper LED-photodiode output signal, and when using the WMS method, it is the 9.5 kHz sinusoidal voltage used to modulate the laser injection current.

In addition to the absorption photodiode, a single, 10 × 10 mm photodiode is used to collect fluorescence from the lithium atoms. This photodiode is located outside of the vacuum chamber, approximately 5 cm above the intersection point of the laser and lithium beams. While not essential for our method, this photodiode is useful when monitoring the chopping of the lithium beam and for frequency calibration of the PZT scan.

Calibration of the PZT scan is needed to infer the atomic beam density when using either the chopped beam or the WMS methods and we use an optical sideband technique for this calibration. The laser injection current is modulated at an accurately known frequency (f_{sb}) which imprints sidebands on the laser spectrum at frequencies $f_0 \pm f_{sb}$, where f_0 is the laser frequency without modulation. Typically $f_{sb} = 170$ MHz and this frequency is measured to an accuracy of 10 ppm by a Fluke PM6685 frequency counter. The laser frequency is scanned across the $2S_{1/2}$, $F = 2 \rightarrow 2P_{3/2}$ resonance using the PZT, and atomic fluorescence is detected, as shown in Fig. 2. Three distinct peaks are observed, one for each of the two sideband lasing frequencies and one for the main lasing frequency, f_0. Since the frequency separation of the peaks is accurately known, they provide a three-point, linear calibration for the scan. This calibration procedure is repeated periodically throughout course of an experimental run lasting

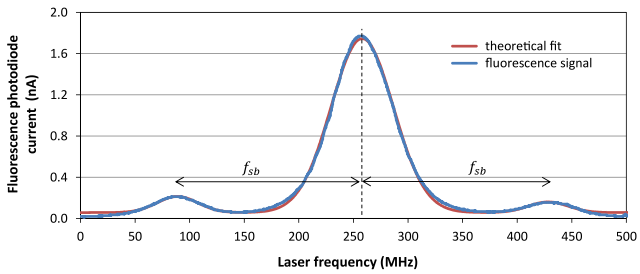

FIG. 2. Detected atomic fluorescence as the laser with optical sidebands is scanned across the resonance transition in lithium. The separation of the optical sidebands (f_{sb}) is accurately known and provides a frequency calibration for the scan. The theoretical fit includes an offset to account for background light reaching the photodiode and so does not fall to zero at the extremes of the scan.

many hours and these repeated measurements give scan rates which have a typical standard error of 0.4%.

III. RESULTS AND DISCUSSION

A. Chopped beam method

The theoretical basis for our technique is the Beer-Lambert law for the absorption of light by a sample of atoms,[44]

$$I_T(\nu) = I_0(\nu)e^{-\sigma(\nu)\int ndz} \approx I_0(\nu)\left(1-\sigma(\nu)\int ndz\right), \quad (1)$$

where ν is the frequency of the laser light, $I_T(\nu)$ is the intensity of laser light transmitted through the atoms, $I_0(\nu)$ is the laser intensity incident upon the atoms, $\sigma(\nu)$ is the absorption cross section, and n is the density of atom absorbers, which is integrated along the path of the laser light (the z direction). The approximation of the exponential function in Eq. (1) is valid for low absorptions (the exponential and its approximation differ by 0.005% for a fractional absorption of 1%), and the equation is valid provided the laser intensity is well below saturation.[45] The frequency dependent absorption cross section is given by[46]

$$\sigma(\nu) = \left(\frac{g_2}{g_1}\right)\left(\frac{A_{21}\lambda^2}{8\pi}\right)\chi(\nu), \quad (2)$$

where g_1 and g_2 are the degeneracies of the lower and upper atomic states involved in the transition, A_{21} is the spontaneous emission rate, and $\chi(\nu)$ is the area-normalized lineshape function. Combining Eqs. (1) and (2) and rearranging give

$$\left(\frac{g_2}{g_1}\right)\left(\frac{A_{21}\lambda^2}{8\pi}\right)\left(\int ndz\right)\chi(\nu) = \frac{I_0(\nu)-I_T(\nu)}{I_0(\nu)} \quad (3)$$

and integrating Eq. (3) over all laser frequencies, ν, leads to

$$\left(\frac{g_2}{g_1}\right)\left(\frac{A_{21}\lambda^2}{8\pi}\right)\int ndz = \int \frac{I_0(\nu)-I_T(\nu)}{I_0(\nu)}\,d\nu = \int \frac{V_0(\nu)-V_T(\nu)}{V_0(\nu)}\,d\nu. \quad (4)$$

The absorption photodiode voltages $V_0(\nu)$ and $V_T(\nu)$ are proportional to the laser intensities $I_0(\nu)$ and $I_T(\nu)$, and the quantity $V_0(\nu) - V_T(\nu)$ is determined by the lock-in amplifier while the atomic beam is being chopped. The measured lock-in amplifier voltage, $V_{LIA}(\nu)$, is proportional to $V_0(\nu) - V_T(\nu)$,

$$V_{LIA}(\nu) = \frac{c_1}{2\sqrt{2}}\left(V_0(\nu)-V_T(\nu)\right), \quad (5)$$

where c_1 is the Fourier coefficient of the first harmonic of the photodiode signal. If this signal were sinusoidal, c_1 would equal 1. Therefore, in terms of known constants and measured voltages, the density of the atomic beam is calculated from

$$\int ndz = \left(\frac{g_1}{g_2}\right)\left(\frac{8\pi}{A_{21}\lambda^2}\right)\left(\frac{2\sqrt{2}}{c_1 V_0}\right)\int V_{LIA}(\nu)\,d\nu. \quad (6)$$

In our experiments, the laser intensity varies by only 0.25% over the course of a scan and so $V_0(\nu)$ can be considered independent of frequency. It is therefore taken out of the integral in Eq. (6) and replaced with V_0. Once a value for c_1 is determined, Eq. (6) is used to establish the integrated atomic beam density.

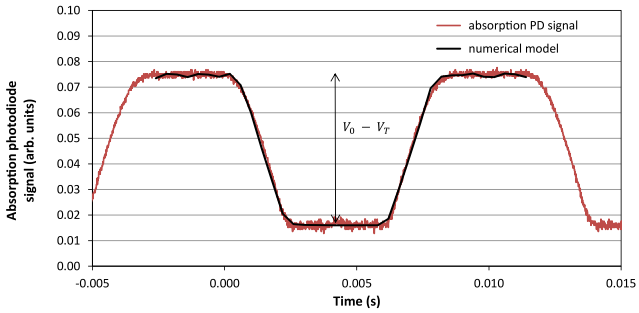

FIG. 3. Absorption photodiode signal recorded while the atomic beam chopper is rotating (red points) and the calculated absorption signal based on a 7.1 mm thick atomic beam (black line). The signal corresponds to the absorption of 0.02.

We have determined c_1 both experimentally and theoretically. Experimental absorption data, taken while the atomic beam is chopped, are shown in Fig. 3. Due to the finite thickness of the lithium atomic beam (7.1 mm at the location of the chopper), the turning on and off of the atomic beam is not instantaneous and the resultant time-profile has a trapezoidal shape, as seen. The quantity c_1 is easily found by taking the ratio of measured values at a fixed laser frequency,

$$c_1 = \frac{2\sqrt{2}V_{LIA}}{V_0 - V_T}, \quad (7)$$

where $V_0 - V_T$ is determined from the absorption photodiode signal shown in Fig. 3, and V_{LIA} is the voltage recorded by the lock-in amplifier connected to the absorption photodiode. A value of $c_1 = 1.16$ is determined for our experimental situation.

This method of finding c_1 can be used as long as the atomic absorption is large enough that $V_0 - V_T$ can be measured accurately. With our apparatus, this translates to absorbed fractions of order 10^{-3} or higher before noise begins to compromise the signal, $V_0 - V_T$. For lower absorptions, fluorescence data can provide a higher signal to noise ratio. Alternatively, a numerical calculation can be used. Figure 3 shows such a calculation (solid black line), which matches the experimental results well. In the calculation, a velocity distribution appropriate for an atomic beam[3] is used to calculate the arrival times of individual atoms at the laser-atom intersection point as the chopper edge cuts across the atom beam. This calculation can be made for any atomic beam temperature, chop frequency, or separation distance between the chopper and the absorption laser. Once the chopped beam profile has been calculated, the coefficient c_1 can be inferred by Fourier analysis. In this way, c_1 can be determined for any particular experimental configuration.

A simpler method of estimating c_1 can be made by assuming a trapezoidal shape for the time-varying absorption profile which allows c_1 to be determined from an analytical formula. A trapezoidal waveform is defined by its period, T, the duration of time the trapezoid is at its low value, T_{low}, and the transition time, T_Δ, between the low and the high values. These times are easily calculated if one knows the atomic beam width and the geometry and speed of the chopper and

can be used to determine c_1 from

$$c_1 = \frac{4}{\pi^2}\frac{T}{T_\Delta}\sin\left[\frac{\pi T_\Delta}{T}\right]\sin\left[\frac{\pi}{T}(T_\Delta + T_{low})\right]. \quad (8)$$

We have found Eq. (8) to agree with our experimental value to within 6%.

As mentioned above, Eq. (1) is only valid at laser intensities well below saturation, and so accurate density measurements require rather low laser powers. Low laser power also ensures that optical pumping effects are negligible. Were this not the case, the analysis used to determine the atomic density with the chopped beam or WMS methods would be significantly more complicated. To determine how low a laser power is needed, Fig. 4 shows measurements of the absorption on resonance, α_{pk}, as a function of laser power. As is seen in the figure appropriately low laser powers are those below about 10 μW where the absorption curve has plateaued. In our density measurements, laser powers less than 7 μW are used, corresponding to intensities $<0.02 I_{sat}$.

Typical absorption data used to determine beam density are shown in Fig. 5. A single Gaussian is used to fit the experimental data, which is then integrated over frequency to give the lithium density from Eq. (6). In Eq. (6), a value of 3.6898×10^7 s^{-1} is used for A_{21},[49,50] and the ratio of the degeneracies of the $2S_{1/2}$, $F = 2$ and the $2P_{3/2}$, $F = 1, 2, 3$ states involved in the transition is $\frac{g_1}{g_2} = \frac{1}{3}$, while the vacuum wavelength of the transition is 670.96201 nm.[24] These values lead to a line-of-sight integrated lithium density of 2.78×10^7 cm^{-2} for the data in Fig. 5. All densities quoted here are the density of atoms in the $2S_{1/2}$, $F = 2$ ground state. The total density of lithium atoms (including those in the $2S_{1/2}$, $F = 1$ ground state) is a factor of $\frac{8}{5}$ larger.

Lineshape fit functions other than a single Gaussian were investigated. A pseudo-Voigt profile using the known natural linewidth of the transition did not lead to an improved fit, neither did including three overlapping lineshape functions (Gaussian or pseudo-Voigt) separated by the known hyperfine intervals of the $2P_{3/2}$ state. Numerical integration of the data was also performed, but a single Gaussian, as the simplest lineshape function, was chosen as the standard fit function for the calculations presented here. The uncertainty in measured density due to the choice of fit function is discussed in Section III D.

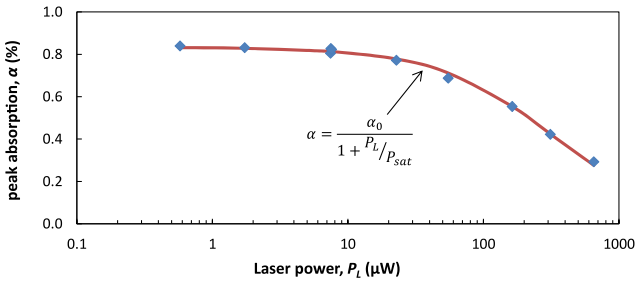

FIG. 4. Resonant absorption depends on laser power due to saturation of the atomic transition. Powers under 10 μW ensure saturation effects are negligible. A fit to the data, using the expected variation of peak absorption with laser power[47] (red line), gives a saturation intensity of 5.3 mW/cm^2, consistent with previous work.[48]

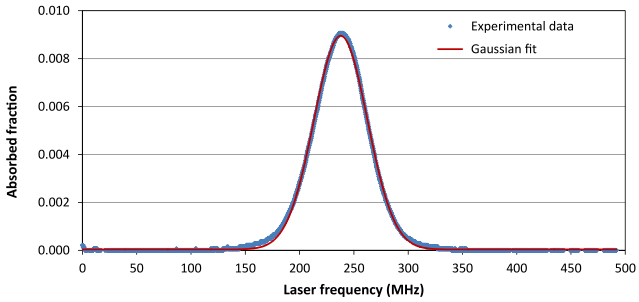

FIG. 5. Absorption data using the chopped beam method for a lithium beam produced at an oven temperature of 462 °C. At this temperature the lithium beam absorbs almost 1% of resonant laser light. Integrating the Gaussian fit curve over frequency gives a lithium density of 2.78×10^7 cm^{-2}.

Figure 6 shows the absorption from a much less intense beam, when the oven was at a temperature of 314 °C. The small but measureable peak absorption ($\sim 2 \times 10^{-5}$) illustrates the sensitivity of our method to determine atomic beam densities. In Fig. 6 the integrated lithium density is 4.4×10^4 cm^{-2}, or an average beam density of 4.9×10^4 cm^{-3} for a 0.9 cm thick beam. The limiting factor in the measurement is the presence of 60 Hz pickup in the absorption detector and cabling connecting the detector to the lock-in amplifier. This pickup, when mixed with the 87 Hz lock-in reference frequency, leads to a 27 Hz background signal which must be filtered by the lock-in amplifier output filter. A long time-constant filter provides greater attenuation of the background, but slows the measurement since it requires a slower scan rate. This constraint on the scan rate is not, however, particularly restrictive because, while a long time-constant filter will broaden the peak of the spectrum and reduce its amplitude, the area under the peak (and therefore the measured density) remains unchanged. When collecting the data shown in Fig. 6, a 3 ms time constant lock-in output filter was used and the data are an average of 64 oscilloscope scans, taking a total time of 70 s. The density of stronger atomic beams, such as that which gave the data shown in Fig. 5, can be measured in 1 s, illustrating the use of our method for real-time beam density monitoring.

The data shown in Fig. 6 used the "double beam" technique with both the atoms and reference channel laser beams present. To illustrate the improvement that is gained by

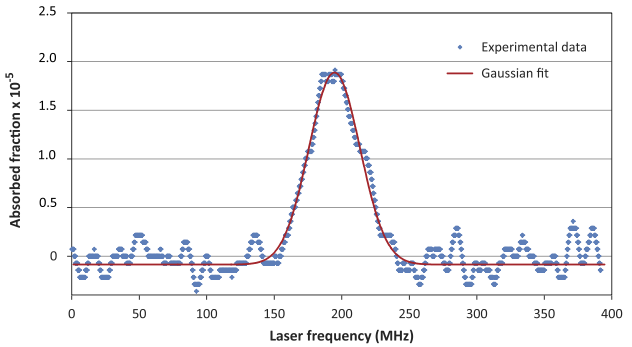

FIG. 6. Absorption data from a low-density lithium beam using the chopped beam method. Despite the small absorption, the absorption peak is still clearly visible.

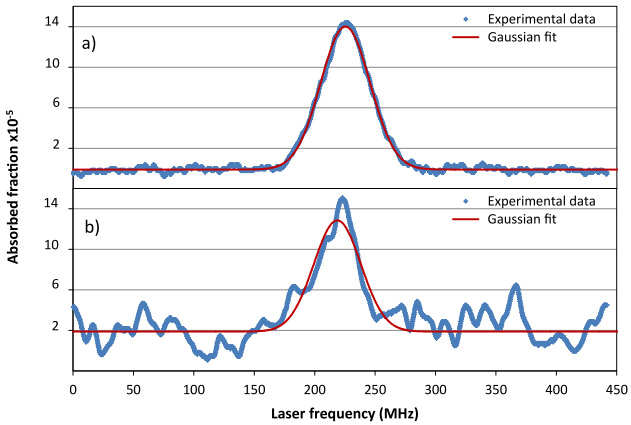

FIG. 7. Absorption data for a lithium beam using (a) the double laser beam technique and (b) using a single laser beam. Common mode noise is rejected by the double beam method giving a larger signal to noise ratio.

using both channels, Fig. 7 shows the absorption spectra from a relatively weak atomic beam when the reference channel is open and when it is blocked. The improvement with an open reference channel is clear. When probing beams with absorptions greater than 0.1%, there is sufficient signal so that the double beam technique is not required.

B. Wavelength modulation spectroscopy method

To provide confirmation of our density measurements using the chopped beam method, we used our experimental setup to determine the beam density with the technique of wavelength modulation spectroscopy (WMS). This is a sensitive technique used to monitor atomic or molecular species found in plasmas,[51,52] laser or electron-beam ablation plumes,[53,54] furnaces,[55,56] and to measure the presence of trace elements in gases.[57–60] The atomic beam is not chopped while the density is measured with the WMS technique and so the details provided below may be useful in experimental situations where chopping the beam is undesirable.

When measuring density using WMS, the laser beam is again passed through the atomic sample and onto a photodiode detector. The frequency of the laser is modulated sinusoidally by modulating the laser injection current at a frequency f_{mod} which also has the (undesirable) effect of modulating the laser intensity. While the modulation is applied, the laser frequency is scanned slowly across the atomic resonance and the photodiode signal is sent to a lock-in amplifier which measures the signal at the modulation frequency and its second harmonic. These signals are used to determine the line-integrated atomic density, as described below. More complex WMS techniques using signal detection at higher harmonics of the modulation frequency have also been employed.[43,61–64]

The starting point for analysis of WMS signals is Eq. (1),

$$I_T(\nu) = I_0(\nu)e^{-\sigma(\nu)\int ndz} \approx I_0(\nu)\left(1-\sigma(\nu)\int ndz\right) = I_0(\nu)\left(1-\sigma_0\overline{\chi}(\nu)\int ndz\right), \tag{9}$$

where we have introduced the absorption cross section on resonance, σ_0, and the peak-normalized lineshape function, $\overline{\chi}(\nu)$. When the laser current is modulated, both frequency modulation (FM) and laser intensity or amplitude modulation (AM) occurs,

$$\text{FM:} \quad \nu = \nu_L + \delta\nu\cos(\omega t - \psi), \tag{10}$$

$$\text{AM:} \quad I_0(\nu) = I(\nu_L) + \Delta I(\nu_L)\cos(\omega t), \tag{11}$$

where υ_L is the laser center frequency, $\delta\nu$ is the FM amplitude, $\Delta I(\nu_L)$ is the amplitude of the intensity modulation, $\omega = 2\pi f_{\mathrm{mod}}$, and ψ is the phase difference between the FM and AM. In our experiments with $f_{\mathrm{mod}} = 9.5$ kHz, the phase difference is measured to be 4° and the lock-in amplifier phase is chosen to maximize the FM signals. Combining Eqs. (9) and (11) gives

$$I_T(\nu) = [I(\nu_L) + \Delta I(\nu_L)\cos(\omega t)]\left(1-\sigma_0\overline{\chi}(\nu)\int ndz\right). \tag{12}$$

If the FM amplitude, $\delta\nu$, is small compared to the transition linewidth, a Taylor series expansion of the lineshape function can be used,

$$\begin{aligned}\overline{\chi}(\nu) &= \overline{\chi}(\nu_L) + \overline{\chi}'(\nu_L)(\nu-\upsilon_L) + \frac{1}{2}\overline{\chi}''(\nu_L)(\nu-\nu_L)^2 + \cdots \\ &= \overline{\chi}(\nu_L) + \overline{\chi}'(\nu_L)\delta\nu\cos(\omega t-\psi) \\ &\quad + \frac{1}{2}\overline{\chi}''(\nu_L)(\delta\nu)^2\cos^2(\omega t-\psi) + \cdots,\end{aligned} \tag{13}$$

where $\overline{\chi}'$ and $\overline{\chi}''$ are derivatives of the lineshape function with respect to laser frequency and Eq. (10) has been used. Finally, combining Eqs. (12) and (13) leads to

$$\begin{aligned}I_T(\nu) &= I(\nu_L)\left(1-\sigma_0\overline{\chi}(\upsilon_L)\int ndz\right) + \Delta I(\nu_L)\cos(\omega t) \\ &\quad - \Delta I(\nu_L)\sigma_0\overline{\chi}(\nu_L)\left(\int ndz\right)\cos(\omega t) \\ &\quad - I(\nu_L)\sigma_0\overline{\chi}'(\nu_0)\delta\nu\left(\int ndz\right)\cos(\omega t-\psi) \\ &\quad - \frac{1}{2}\Delta I(\nu_L)\sigma_0\overline{\chi}'(\nu_0)\delta\nu\left(\int ndz\right)\cos(2\omega t-\psi) \\ &\quad - \frac{1}{4}I(\nu_L)\sigma_0\overline{\chi}''(\nu_L)(\delta\nu)^2\left(\int ndz\right) \\ &\quad \times\cos(2\omega t-2\psi)+\cdots.\end{aligned} \tag{14}$$

The first term on the right hand side of Eq. (14) is a d.c. term, while the other terms represent signals at the fundamental and second harmonic of the modulation frequency, ω, and are known as the $1f$ and $2f$ signals. Higher order terms exist in Eq. (14), but are negligible if the modulation amplitude, $\delta\nu$, is kept below about 10% of the full-width at half maximum of the transition.[65] The density of the atomic beam can be determined from measurements of either the $1f$ or the $2f$ signals, once the modulation amplitude, $\delta\nu$, and lineshape functions are known.

Time-varying terms in Eq. (14) which are proportional to $\Delta I(\nu_L)$ are AM terms, and those proportional to $I(\nu_L)$ are FM terms. In our work, we use the FM terms to determine the atomic density since they are much larger than the density-dependent AM terms. The density-independent AM term, $\Delta I(\nu_L)\cos(\omega t)$, can, however, be large enough to limit the

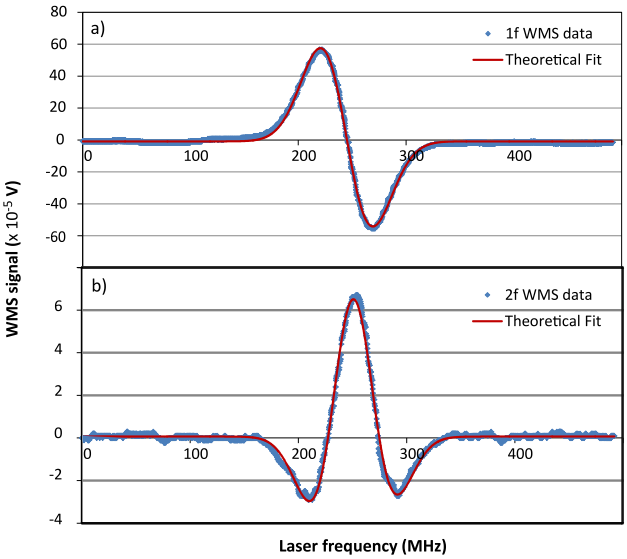

FIG. 8. Typical 1f and 2f WMS signals used to determine lithium beam density, which for this data set is 2.8×10^7 cm^{-2}.

usable sensitivity setting of our lock-in amplifier unless the double-beam technique is used to cancel its contribution.

Typical $1f$ and $2f$ signals measured by our lock-in amplifier are shown in Fig. 8. The frequency variation of the signals is the expected first and second derivative of a Gaussian lineshape since the FM signals provide the dominant contribution. Were the double beam method not used, the $1f$ signal would show a large d.c. offset. The fit functions we use for the two signals are, for the $1f$ signal,

$$A_1\overline{\chi}(\nu) + B_1\overline{\chi}'(\nu) + C_1 \tag{15}$$

and for the $2f$ signal,

$$A_2\overline{\chi}'(\nu) + B_2\overline{\chi}''(\nu) + C_2. \tag{16}$$

The C_1 term accounts for imperfect cancellation of the $\Delta I(\nu_L)\cos(\omega t)$ contribution and the C_2 term accommodates a possible $2f$ offset caused by any non-linear AM response of the laser diode to the current modulation. As can be seen in Fig. 8, these offsets are approximately zero. A_1 and A_2 are the amplitudes of the density-dependent AM signals, and in our work, these also contribute little to the signal. The fit coefficients B_1 and B_2 represent the contributions of the FM signals to the total $1f$ and $2f$ signals, and the modulation amplitude, $\delta\nu$, can be found from their ratios,

$$\frac{B_2\overline{\chi}''}{B_1\overline{\chi}'} = \frac{-\frac{1}{4}I(\nu_L)\sigma_0\overline{\chi}''(\nu_L)(\delta\nu)^2\left(\int n dz\right)}{-I(\nu_L)\sigma_0\overline{\chi}'(\nu_L)\delta\nu\left(\int n dz\right)} \tag{17}$$

which gives

$$\delta\nu = 4\frac{B_2}{B_1}. \tag{18}$$

This relationship is true generally, independent of the actual lineshape function. Using either the $1f$ or the $2f$ FM terms in Eq. (14), equating them with their corresponding term in Eqs. (15) and (16), and using Eq. (18), one finds

$$\int n\,dz = \frac{\sqrt{2}B_1^2}{4V_0\sigma_0 B_2}. \tag{19}$$

The quantity V_0 represents the output voltage of the absorption photodiode with no atomic beam present, as before, and the $\sqrt{2}$ converts the r.m.s. voltage measured by the lock-in amplifier to a voltage amplitude. Finally, including the explicit expression for σ_0 for a Gaussian lineshape gives

$$\int n\,dz = \sqrt{\frac{8\pi^3}{\ln(2)}}\frac{1}{V_0}\frac{B_1^2}{B_2}\frac{g_1}{g_2}\frac{\gamma}{\lambda^2 A_{21}} = 3.80\times10^5\frac{\gamma}{V_0}\frac{B_1^2}{B_2}, \tag{20}$$

where γ is the Gaussian half-width at half maximum, and the numerical constant is appropriate for the transition in lithium we are studying. When using the WMS method, beam densities are calculated from Eq. (20) after fits to the $1f$ and $2f$ data provide values for B_1, B_2, and γ.

C. Comparison of methods

Comparisons between atomic densities measured using the chopped beam and the WMS methods were made in two situations. First, after the lithium oven had been at operating temperature for several hours, a series of four sets of 25 density measurements were made, half of which used the WMS method and half used the chopped beam method, as shown in Fig. 9. Since fits to the $1f$ and $2f$ WMS spectra gave slightly different Gaussian half-widths, each WMS dataset shows two values for the beam density, one using the half-width found from fitting the $1f$ spectrum and the other using the $2f$ fitted half-width. It can be seen that the density measurements made with the chopped beam method fall between the WMS values. The chopped beam method measurements display less scatter than the WMS results by a factor of two, probably due to the better signal to noise of the chopped beam data (compare Figs. 5 and 8(b)). The chopped beam and both WMS datasets show an increase in atomic density of 2% in the 25 min time period between the two sets of 25 measurements. This is due to the fact that the oven temperature had not perfectly stabilized when the data were taken. On average, the chopped beam measurements give beam densities 1.8% below the $1f$ WMS measured values and 4.5% above the WMS $2f$ value. Averaging the $1f$ and $2f$ WMS data together, the chopped beam measured densities are 1.2% higher than the WMS densities. As further comparison between chopped beam and WMS methods, Fig. 10 shows data taken as the oven is cooling

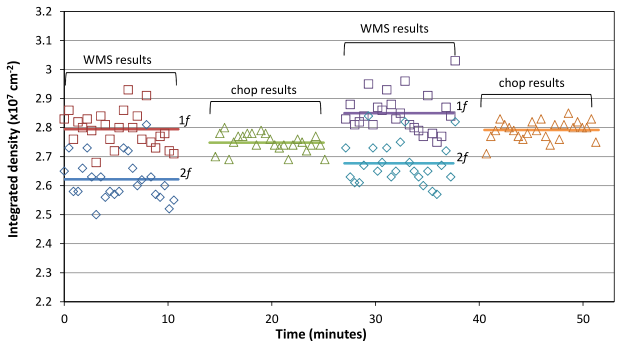

FIG. 9. Comparison of lithium beam densities determined using the chopped beam and WMS methods shows good agreement. For the WMS technique, the density can be determined using either the 1f or the 2f half-widths. The solid lines represent the average of each set of 25 measurements.

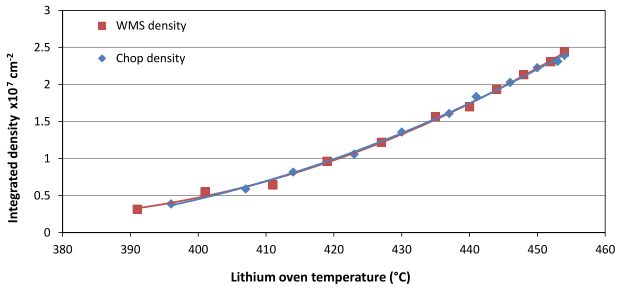

FIG. 10. Comparison of the lithium densities determined by the chopped beam and the 1f WMS methods, taken as the lithium oven was allowed to cool.

from its operating temperature. It can be seen that the two sets of data are virtually indistinguishable.

D. Chopped beam method sensitivity, accuracy, and precision

As seen in Fig. 6, the chopped beam method is sensitive to fractional absorptions of order 10^{-5}. Since 60 Hz pickup is the dominant background for our measurements, it is likely that this sensitivity could be improved by employing a higher chop frequency than our value of 87 Hz. The accuracy of density measurements made using the chopped beam method is inferred from the close agreement with densities measured using the WMS technique. Given the data shown in Figs. 9 and 10, we are confident that an accuracy of better than 5% has been achieved.

The precision of the density measurements made with the chopped beam method is determined by several factors, summarized in Table I.

The dominant uncertainty is the choice of lineshape function used to fit the experimental data. Single Gaussian, single pseudo-Voigt, triple Gaussian, triple pseudo-Voigt, and interpolating functions were used as fit functions. A sample of experimental data taken over a 3 month period was fit using these different functions and 90% of the densities determined fell within 2.6% of the density values found using a single Gaussian fit function. This value of 2.6% was therefore taken as the uncertainty due to the choice of lineshape function.

The instrument uncertainty in Table I accounts for the accuracies of the lock-in amplifier used to measure V_{LIA} and the voltage meter used to measure V_0, and is taken from the manufacturer specifications for these instruments. The uncertainties are combined in quadrature to give a total instrumental uncertainty of 1.1%. The next largest uncertainty is that of the constant c_1. This constant is measured as described above, and repeated measurements gave a standard error of 0.9% or equivalently a 0.9% uncertainty in the inferred density. The uncertainty in density measurements due to uncertainties in calibrating the PZT frequency scan has two sources of error. First, repeated measurements of the scan rate over the course of many hours show a 0.42% standard error. Second, our calibration assumes that the frequency scan is linear in time. If instead, a quadratic time variation is assumed, there is at most a 0.2% change in the measured density values. Combining these two uncertainties in quadrature results in a total uncertainty of 0.5% due to the frequency calibration. The final contribution shown in Table I is the 0.3% standard error for repeated measurements of the density shown in Fig. 9. A total uncertainty in our density measurements is found by combining in quadrature the separate contributions in Table I and leads to an ultimate precision of 3%. Since the dominant uncertainty is due to the choice of lineshape function and 90% of density measurements fell within this uncertainty, we likewise estimate that 90% of density measurements will fall within the final uncertainty of 3%.

TABLE I. Contributions to the uncertainty of the chopped beam method for measuring density.

Source	Percentage uncertainty
Lineshape fit function	2.6
Instrument	1.1
Statistical variation in c_1 measurements	0.9
Frequency calibration	0.5
Statistical variation in density measurements	0.3
Total uncertainty	3.0

IV. CONCLUSION

Laser absorption spectroscopy of a chopped lithium beam has been used to measure the atomic beam density, integrated along the path of the laser. Our technique can be applied to any atomic or molecular species for which a suitable laser wavelength can be generated and could also be used to measure the density of metastable state atoms. The requirements for laser power are minimal since intensities well below saturation are required.

For beams which absorb of order 1% of the laser light, we have shown that the precision and accuracy of our measurements are better than 5% and can be made in real time. In addition, the sensitivity of our method allows it to be applied to atomic beams with fractional absorptions as low as 10^{-5}. We anticipate that our technique with its demonstrated precision will be applicable to a range of different experiments, including those which use an atomic or molecular beam as a collision target.

ACKNOWLEDGMENTS

We would like to thank Professor Timothy Roach for advice and for the loan of equipment during our work. We also thank the Richard B. Fisher'47 Summer Research Fellowship Program at the College of the Holy Cross for funding.

[1]W. Gerlach and O. Stern, Z. Phys. **9**, 353 (1922).
[2]W. H. Rodebush, Rev. Mod. Phys. **3**, 392 (1931).
[3]N. Ramsey, *Molecular Beams* (Oxford University Press, 1985).
[4]C. B. Lucas, *Atomic and Molecular Beams: Production and Collimation* (CRC Press, 2013).
[5]C. Havener, M. Huq, H. Krause, P. Schulz, and R. Phaneuf, Phys. Rev. A **39**, 1725 (1989).
[6]F. Aumayr, M. Gieler, H. Winter, and J. Schweinzer, J. Phys. B: At., Mol. Opt. Phys. **29**, 1515 (1996).
[7]D. Fisher, S. Lundeen, C. Fehrenbach, and B. DePaola, Phys. Rev. A **63**, 052712 (2001).

[8]K. Nagesha and K. MacAdam, Phys. Rev. Lett. **91**, 113202 (2003).
[9]W. Chen, G. Vorobyev, D. Guo, P. Hillenbrand, F. Herfurth, S. Hagmann, U. Spillmann, S. Trotsenko, A. Gumberidze, and T. Stöhlker, Phys. Rev. A **88**, 052703 (2013).
[10]R. Isler, Plasma Phys. Controlled Fusion **36**, 171 (1994).
[11]R. Brandenburg, J. Schweinzer, S. Fiedler, F. Aumayr, and H. Winter, Plasma Phys. Controlled Fusion **41**, 471 (1999).
[12]Z. Herman, Int. J. Mass Spectrom. **212**, 413 (2001).
[13]I. H. Hutchinson, Plasma Phys. Controlled Fusion **44**, 2603 (2002).
[14]S. Medley, A. Donné, R. Kaita, A. Kislyakov, M. Petrov, and A. Roquemore, Rev. Sci. Instrum. **79**, 011101 (2008).
[15]M. Reich, E. Wolfrum, J. Schweinzer, H. Ehmler, L. Horton, J. Neuhauser, and A. U. Team, Plasma Phys. Controlled Fusion **46**, 797 (2004).
[16]L. Grisham, Phys. Plasmas **14**, 102509 (2007).
[17]W. D. Phillips and H. Metcalf, Phys. Rev. Lett. **48**, 596 (1982).
[18]A. Aspect, E. Arimondo, R. Kaiser, N. Vansteenkiste, and C. Cohen-Tannoudji, Phys. Rev. Lett. **61**, 826 (1988).
[19]G. Timp, R. Behringer, D. Tennant, J. Cunningham, M. Prentiss, and K. Berggren, Phys. Rev. Lett. **69**, 1636 (1992).
[20]H. J. Metcalf and P. Van der Straten, *Laser Cooling and Trapping, Graduate Texts in Contemporary Physics* (Springer, New York, 1999).
[21]D. Meschede and H. Metcalf, J. Phys. D **36**, R17 (2003).
[22]B. Smeets, P. van der Straten, T. Meijer, C. Fabrie, and K. van Leeuwen, Appl. Phys. B **98**, 697 (2010).
[23]C. J. Sansonetti, B. Richou, R. Engleman, Jr., and L. J. Radziemski, Phys. Rev. A **52**, 2682 (1995).
[24]C. J. Sansonetti, C. Simien, J. D. Gillaspy, J. N. Tan, S. M. Brewer, R. C. Brown, S. Wu, and J. V. Porto, Phys. Rev. Lett. **107**, 023001 (2011).
[25]J. Borbely, M. George, L. Lombardi, M. Weel, D. Fitzakerley, and E. Hessels, Phys. Rev. A **79**, 060503 (2009).
[26]C. G. Parthey, A. Matveev, J. Alnis, B. Bernhardt, A. Beyer, R. Holzwarth, A. Maistrou, R. Pohl, K. Predehl, and T. Udem, Phys. Rev. Lett. **107**, 203001 (2011).
[27]E. Peters, S. Reinhardt, T. W. Hänsch, and T. Udem, Phys. Rev. A **92**, 063403 (2015).
[28]N. Rothery, C. Storry, and E. Hessels, Phys. Rev. A **51**, 2919 (1995).
[29]K. MacAdam, J. Day, J. Aguilar, D. Homan, A. MacKellar, and M. Cavagnero, Phys. Rev. Lett. **75**, 1723 (1995).
[30]M. Huang, M. Stöckli, C. Fehrenbach, S. Lundeen, and B. DePaola, J. Phys. B: At., Mol. Opt. Phys. **30**, 2425 (1997).
[31]C. S. Hwang and K. MacAdam, Phys. Rev. A **68**, 042709 (2003).
[32]T. F. Gallagher, *Rydberg Atoms* (Cambridge University Press, 2005).
[33]T. M. Roach and D. Henclewood, J. Vac. Sci. Technol., A **22**, 2384 (2004).
[34]Y. Bruneau, G. Khalili, P. Pillet, and D. Comparat, Eur. Phys. J. D **68**, 1 (2014).
[35]C. Burkhardt, J. Libbert, J. Xu, J. Leventhal, and J. Kelley, Phys. Rev. A **38**, 5949 (1988).
[36]N. Schofield, D. Paganin, and A. Bishop, Rev. Sci. Instrum. **80**, 123105 (2009).
[37]N. Ahmed, A. Nadeem, M. Nawaz, S. Bhatti, M. Iqbal, and M. Baig, Rev. Sci. Instrum. **76**, 063105 (2005).
[38]B. M. Patterson, J. F. Sell, T. Ehrenreich, M. A. Gearba, G. M. Brooke, J. Scoville, and R. J. Knize, Phys. Rev. A **91**, 012506 (2015).
[39]C. Ching, J. Bailey, P. Lake, A. Filuk, R. Adams, and J. McKenney, Rev. Sci. Instrum. **68**, 354 (1997).
[40]A. Dinklage, T. Lokajczyk, H. Kunze, B. Schweer, and I. Olivares, Rev. Sci. Instrum. **69**, 321 (1998).
[41]A. Christmann, S. Seidel, and H. Kunze, Rev. Sci. Instrum. **70**, 1627 (1999).
[42]A. Camposeo, A. Piombini, F. Cervelli, F. Tantussi, F. Fuso, and E. Arimondo, Opt. Commun. **200**, 231 (2001).
[43]P. Kluczynski, J. Gustafsson, Å. M. Lindberg, and O. Axner, Spectrochim. Acta, Part B **56**, 1277 (2001).
[44]W. Demtröder, *Laser Spectroscopy: Basic Concepts and Instrumentation* (Springer-Verlag, 1996), p. 65.
[45]R. C. Hilborn, Am. J. Phys. **50**, 982 (1982).
[46]C. J. Foot, *Atomic Physics* (Oxford University Press, 2004), p. 140.
[47]M. Inguscio and L. Fallani, *Atomic Physics: Precise Measurements and Ultracold Matter* (Oxford University Press, 2013), p. 261.
[48]C. Iu, G. D. Stevens, and H. Metcalf, Appl. Opt. **34**, 2640 (1995).
[49]Z. Yan and G. W. Drake, Phys. Rev. A **52**, R4316 (1995).
[50]W. McAlexander, E. Abraham, and R. Hulet, Phys. Rev. A **54**, R5 (1996).
[51]A. Zybin, C. Schnürer-Patschan, and K. Niemax, J. Anal. At. Spectrom. **10**, 563 (1995).
[52]G. Hancock, V. Kasyutich, and G. Ritchie, Appl. Phys. B **74**, 569 (2002).
[53]W. Wang, R. Hammond, M. Fejer, S. Arnason, M. Beasley, M. Bortz, and T. Day, Appl. Phys. Lett. **71**, 31 (1997).
[54]W. Wang, R. Hammond, M. Fejer, and M. Beasley, J. Vac. Sci. Technol., A **17**, 2676 (1999).
[55]J. Liu, J. Jeffries, and R. Hanson, Appl. Phys. B **78**, 503 (2004).
[56]A. Zybin, J. Koch, H. Wizemann, J. Franzke, and K. Niemax, Spectrochim. Acta, Part B **60**, 1 (2005).
[57]R. Engelbrecht, Spectrochim. Acta, Part A **60**, 3291 (2004).
[58]B. M. Moeskops, S. Cristescu, and F. M. Harren, Opt. Lett. **31**, 823 (2006).
[59]K. Sun, R. Sur, J. B. Jeffries, R. K. Hanson, T. Clark, J. Anthony, S. Machovec, and J. Northington, Appl. Phys. B **117**, 411 (2014).
[60]W. Wei, J. Chang, Q. Huang, C. Zhu, Q. Wang, Z. Wang, and G. Lv, Appl. Phys. B **118**, 75 (2015).
[61]A. Dharams and A. Bullock, Appl. Phys. B **63**, 283 (1996).
[62]P. Kluczynski and O. Axner, Appl. Opt. **38**, 5803 (1999).
[63]L. Lan, Y. Ding, Z. Peng, Y. Du, Y. Liu, and Z. Li, Appl. Phys. B **117**, 543 (2014).
[64]L. Lan, Y. Ding, Z. Peng, Y. Du, and Y. Liu, Appl. Phys. B **117**, 1211 (2014).
[65]K. Duffin, A. J. McGettrick, W. Johnstone, G. Stewart, and D. G. Moodie, J. Lightwave Technol. **25**, 3114 (2007).

Erratum: “Precision atomic beam density characterization by diode laser absorption spectroscopy” [Rev. Sci. Instrum. 87, 093103 (2016)]

Paul Oxley and Joseph Wihbey
Physics Department, The College of the Holy Cross, Worcester, Massachusetts 01610, USA

(Received 13 June 2016; accepted 20 August 2016; published online 2 September 2016)

[https://doi.org/10.1063/1.4962025]

The authors would like to correct the numerical value of the degeneracy ratio which enters into Equations (6) and (20).

On page 4 of the original paper it states:

> “In Eq. 6 a value of 3.6898×10^7 s^{-1} is used for A_{21} [49-50], the ratio of the degeneracies of the $2S_{1/2}, F = 2$ and the $2P_{3/2}, F = 1, 2, 3$ states involved in the transition is $\frac{g_1}{g_2} = \frac{1}{3}$, while the vacuum wavelength of the transition is 670.96201 nm[24]”

In fact the value of 3.6898×10^7 s^{-1} for A_{21} is appropriate for a transition between the $2S_{1/2}$ and $2P_{3/2}$, states, which have a degeneracy ratio of $\frac{g_1}{g_2} = \frac{1}{2}$. The corrected sentence should therefore read:

> “In Eq. 6 a value of 3.6898×10^7 s^{-1} is used for A_{21} [49-50], the ratio of the degeneracies of the $2S_{1/2}$ and $2P_{3/2}$ states involved in the transition is $\frac{g_1}{g_2} = \frac{1}{2}$, while the vacuum wavelength of the transition is 670.96201 nm[24]”

A numerical value of $\frac{g_1}{g_2} = \frac{1}{2}$, should therefore be used when evaluating Equations (6) and (20). This change does not affect any of the conclusions in the paper, but simply increases all quoted beam densities by a factor of 3/2. The authors apologize for this error.